⌘ *Author's Choice*

THE JOURNAL OF BIOLOGICAL CHEMISTRY VOL. 287, NO. 45, pp. 37926–37938, November 2, 2012

Activation of NF-κB Protein Prevents the Transition from Juvenile Ovary to Testis and Promotes Ovarian Development in Zebrafish*[S]

Received for publication, June 20, 2012, and in revised form, September 14, 2012 Published, JBC Papers in Press, September 17, 2012, DOI 10.1074/jbc.M112.386284

Ajay Pradhan[‡1], Hazem Khalaf[‡1], Scott A. Ochsner[§1], Rajini Sreenivasan[¶1,2], Jarno Koskinen[‡1], Marie Karlsson[‡1], Jesper Karlsson[‡1], Neil J. McKenna[§], László Orbán[¶‖], and Per-Erik Olsson[‡3]**

*From the [‡]Department of Biology, Örebro Life Science Center, School of Science and Technology, Örebro University, SE-701 82 Örebro, Sweden, [§]Department of Molecular and Cellular Biology, Baylor College of Medicine, Houston, Texas 77030, [¶]Department of Reproductive Genomics, Strategic Research Program, Temasek Life Sciences Laboratory, Singapore 117604, [‖]Department of Biological Sciences, National University of Singapore, Singapore 117543, and **Department of Animal Science and Breeding, Georgikon Faculty, University of Pannonia, Keszthely, H-8360 Hungary*

Background: NF-κB is a key regulator of anti-apoptotic processes and plays a role in gonad formation in mammals.
Results: NF-κB activation leads to female-biased sex differentiation in zebrafish.
Conclusion: Anti-apoptotic signaling during the juvenile ovary stage is needed for the maintenance of oocytes in zebrafish.
Significance: Unraveling the regulation of apoptotic processes during gonadal transformation will facilitate understanding the molecular mechanism of zebrafish sex differentiation.

Testis differentiation in zebrafish involves juvenile ovary to testis transformation initiated by an apoptotic wave. The molecular regulation of this transformation process is not fully understood. NF-κB is activated at an early stage of development and has been shown to interact with steroidogenic factor-1 in mammals, leading to the suppression of anti-Müllerian hormone (*Amh*) gene expression. Because steroidogenic factor-1 and Amh are important for proper testis development, NF-κB-mediated induction of anti-apoptotic genes could, therefore, also play a role in zebrafish gonad differentiation. The aim of this study was to examine the potential role of NF-κB in zebrafish gonad differentiation. Exposure of juvenile zebrafish to heat-killed *Escherichia coli* activated the NF-κB pathways and resulted in an increased ratio of females from 30 to 85%. Microarray and quantitative real-time-PCR analysis of gonads showed elevated expression of NF-κB-regulated genes. To confirm the involvement of NF-κB-induced anti-apoptotic effects, zebrafish were treated with sodium deoxycholate, a known inducer of NF-κB or NF-κB activation inhibitor (NAI). Sodium deoxycholate treatment mimicked the effect of heat-killed bacteria and resulted in an increased proportion of females from 25 to 45%, whereas the inhibition of NF-κB using NAI resulted in a decrease in females from 45 to 20%. This study provides proof for an essential role of NF-κB in gonadal differentiation of zebrafish and represents an important step toward the complete understanding of the complicated process of sex differentiation in this species and possibly other cyprinid teleosts as well.

The molecular mechanism of sex determination is unknown in zebrafish (*Danio rerio*). Earlier, neither cytogenetic studies (1, 2) nor comparative analysis of recombination rates between the two sexes (3) nor an array-based genome screen (4) have led to the identification of sex chromosomes. Recently, analysis of genetic linkage maps have revealed the presence of regions associated with sex determination on four chromosomes (5, 6), indicating polygenic sex determination in zebrafish (4–7).

On the other hand, a number of candidate genes with potential role in sexual development have been identified, including Sry-related HMG box gene 9 (*sox9*), anti-Müllerian hormone (*amh*), cytochrome P450, family 19, subfamily A, polypeptide 1a and b (*cyp19a1a* and *b),* nuclear receptor subfamily 5, group A (*nr5a1 a* and *b*), forkhead box protein L2 (*foxl2*), dead end (*dnd*), and factor in germ line α (*figα*) (7–10). Nr5a or steroidogenic factor-1 controls the expression of *sox9*, *cyp19a1a*, and *amh* (7, 10). In mammals, SOX9 is involved in the regulation of Amh[4] (11). In mice, homozygous mutation of Sox9 binding site in *Amh* leads to lack of its transcription and development of pseudohermaphrodites (12), whereas mutations in the *sox9* gene result in sex reversal in XY campomelic dysplasia patients (13).

Zebrafish gonadal differentiation starts with the formation of a juvenile ovarian structure that either matures into adult ovaries or transforms into testes (14, 15). The testis transformation process has been suggested to depend on apoptosis (16). This

* This research was financed by the Swedish Research Council, the Knowledge Foundation, Sweden, and Örebro University (to P. E.-O.) and by the Agri-Food and Veterinary Authority as well as Temasek Life Sciences Laboratory, Singapore (to L. O.).
⌘ *Author's Choice*—Final version full access.
[S] This article contains supplemental Tables 1–3.
The full set of microarray expression data has been deposited in ArrayExpress under the accession number E-MEXP-3249.
[1] These authors have contributed equally.
[2] Present address: Molecular Genetics and Development Division, Prince Henry's Institute of Medical Research, Monash Medical Centre, Clayton, Victoria 3168, Australia.
[3] To whom correspondence should be addressed. Tel.: 46-19-301244; Fax: 46-19-303566; E-mail: per-erik.olsson@oru.se.

[4] The abbreviations used are: AMH, anti-Müllerian hormone; IAP, inhibitor of apoptosis protein; DOC, sodium deoxycholate; NAI, NF-κB activation inhibitor; qRT-PCR, quantitative RT-PCR; I, intermediate; CM, control male; CF, control females.

was further supported by a recent study where mutations in the Fanconi anemia, complementation group L (*fancl*) gene led to germ cell apoptosis and consequently activated the testis development pathway (17). Introducing mutations in the tumor protein p53 (*tp53*) gene counteracted the effect of the *fancl* mutations (17), suggesting a role for apoptosis in this process. In line with this, germ cell numbers are also important for ovarian development and complete absence of germ cells results in development of sterile males (9, 18).

Nuclear factor κ-light-chain-enhancer of activated B cells (NF-κB) is involved in regulation of inflammation, apoptosis, cell growth, and differentiation and can be activated by various physical and chemical factors (19). NF-κB is a protein complex composed of homo- or heterodimers of five members of the Rel family including NF-κB1 (p50), NF-κB2 (p52), Rel A (p65), Rel B, and c-Rel. These proteins are capable of binding one another with different binding specificities resulting in different DNA binding properties. The p65/p50 dimer is the most abundant heterodimeric form present in cells and is involved in transcription activation of a multitude of genes (19, 20). NF-κB subunits are generally sequestered in the cytoplasm by the inhibitor protein IκB. Numerous factors including UV irradiation, stress, cytokine, and free radicals can promote IκB degradation of the IκB/NF-κB complex, allowing the translocation of NF-κB to the nucleus resulting in subsequent induction of the transcription of its target genes (20–22).

NF-κB activation blocks apoptotic processes and promotes cell survival by interacting with the inhibitor of apoptosis protein (IAP) family of genes (23, 24). NF-κB is also known to interact with other nuclear receptors including the glucorticoid and androgen receptor as well as with other proteins to regulate gene expression (25, 26). NF-κB is highly expressed in mammalian Sertoli cells; it is involved in regulation of spermatogenesis (27) and down-regulates the *Amh* gene expression in mammalian testis. This is due to NF-κB interaction with steroidogenic factor-1, which in turn leads to the recruitment of histone deacetylase and suppression of *Amh* gene expression (28). NF-κB is also involved in the interleukin 1- and tumor necrosis factor-α (TNFα)-mediated down-regulation of *Sox9* expression in mouse chondrocytic cells (29).

Zebrafish embryos and larvae are dependent on a functional innate immune system at an early stage of development (≥1 days post fertilization (dpf)). This includes macrophage and neutrophil differentiation (30), indicating that the NF-κB signaling system is present and active before testis transformation. In addition, a study on goldfish has shown that TNFα inhibits testicular testosterone production (31).

The aim of this study was to investigate the possible role of NF-κB in zebrafish sex differentiation. Induction of the NF-κB signaling pathway resulted in up-regulation of inflammatory and anti-apoptotic genes, and this correlated to female-biased sex ratio. In contrast, inhibition of NF-κB resulted in an increased proportion of males. This study demonstrates the involvement of NF-κB signaling in the maintenance of ovarian development and the inhibition of the transformation of juvenile ovaries to adult testis.

EXPERIMENTAL PROCEDURES

Breeding—Adult zebrafish were maintained in a recirculating system (Aquaneering) with a 14-h light/10-h dark cycle. The fish were fed twice a day with newly hatched *Artemia salina* nauplii and commercial flake food (Tetrarubin). The male and female brooders were kept in separate aquaria at 26–27 °C, and they were allowed to breed once a week. The fish handling procedures were approved by the Swedish Ethical Committee in Linköping (Permit 32-10).

Preparation of Heat-killed Bacteria—E. coli MG1655 was grown on Luria-Bertani (LB) agar and incubated at 37 °C overnight. One colony was inoculated into 10 ml of LB broth and incubated on a shaker (200 rpm) at 37 °C overnight. The bacteria were then centrifuged and washed with 5 ml of phosphate-buffered saline (Sigma). The bacterial pellet was resuspended in 2 ml of PBS and killed by heating to 70 °C for 1 h. To ensure 100% bacteria death, 10 μl of the heat-killed suspension was plated and incubated overnight at 37 °C.

NFκB-pGL4 Plasmid Construction—The pGL4 plasmid with promoter-less Luciferase gene and neomycin selection marker was purchased from Promega, and the NFκB cis-element insert was obtained from commercially available pNFκB-Luc plasmid (BD Biosciences). The pGL4 luciferase plasmid and the pNFκB-Luc plasmid were cut with HindIII and KpnI (Fermentas) and gel-purified by using Wizard SV Gel and PCR Clean-Up System (Promega). The NFκB cis-element and the pGL4 luciferase plasmid were ligated using T4 DNA ligase (Fermentas).

Cell Culture and Development of Stably Transfected Cells—ZFL cells were maintained at 28 °C and 3% CO_2 in a humidified incubator in a complex media containing 50% L15 (Invitrogen), 35% DMEM-high glucose (PAA Laboratories), and 15% Ham's F-12 (Invitrogen) supplemented with 5% fetal bovine serum (Hyclone), 15 mM Hepes buffer (Lonza), 0.15 g/liter sodium bicarbonate (Biochrom AG), 50 ng/ml mouse EGF, and 0.01 mg/ml bovine insulin. For stable transfection, ZFL cells were plated in 24-well plates (BD Biosciences) (80,000 cells/well). The next day the cells were transfected with the NFκB-pGL4 plasmid (500 ng/well) using Lipofectamine 2000 (Invitrogen). After 48 h the cells were treated with 1 mg/ml G418 antibiotic (Duchefa Biochemie). Antibiotic-resistant colonies were selected, and the cells were screened for NFκB activity using the Luciferase assay kit (Promega).

ZFL Cell-based Experiments—Before exposure the stably transfected ZFL cells (nZFL) were plated in 24-well plates (80,000 cells/well) and incubated for 16–18 h at 28 °C and 3% CO_2. Wild type ZFL cells were plated in 12-well plates (BD Biosciences) (2×10^5 cells/well) and incubated for 16–18 h at 28 °C and 3% CO_2. The experiments were started by adding heat-killed bacteria at 5×10^6, 1×10^7, 5×10^7, or 1×10^8 colony forming units (cfu)/ml, sodium deoxycholate (DOC) at 200 or 300 μM (Sigma), or 40 nM NF-κB activation inhibitor (NAI) (Calbiochem) prepared in fresh media to the cells. The cells were incubated for 12 h (Luciferase assays) or 24 h (quantitative RT-PCR (qRT-PCR) assays) at 28 °C and 3% CO_2. Detection of luciferase activity was performed using Luciferase assay kit, whereas cells used for qRT-PCR analysis were lysed with TRI-Reagent (Sigma).

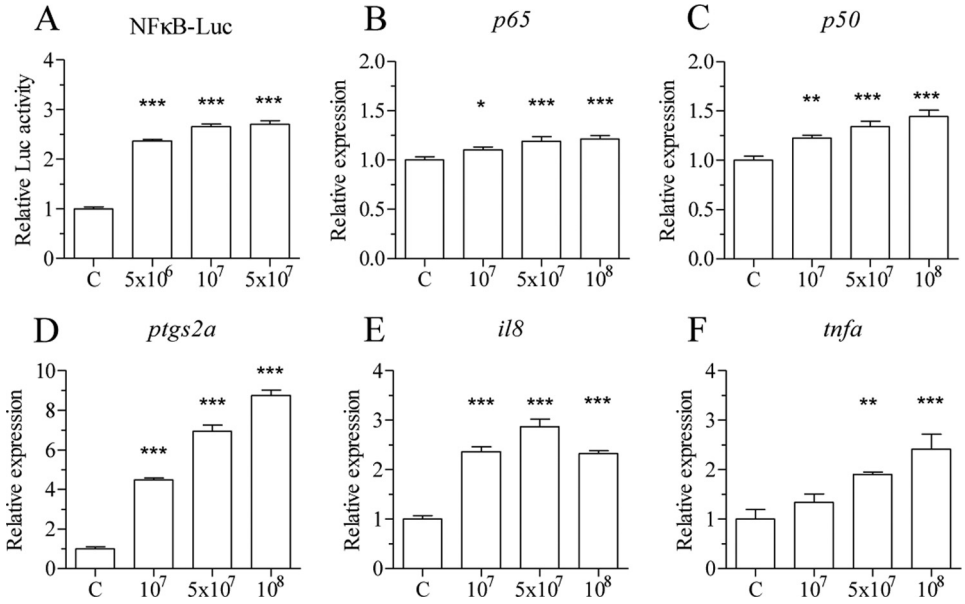

FIGURE 1. **Heat-killed bacteria activate NF-κB and inflammatory genes *in vitro*.** nZFL cells were treated with heat-killed *E. coli* (5×10^6, 1×10^7, and 5×10^7 cfu/ml), and the luciferase activity was determined after 12 h of exposure (*A*). ZFL cells were exposed to heat-killed *E. coli* (1×10^7, 5×10^7, and 1×10^8 cfu/ml) for 24 h, and qPCR analysis was performed to determine *p65* (*B*), *nfkb1/p50* (*C*), *ptgs2a* (*D*), *il8* (*E*) and *tnfa* (*F*). One-way analysis of variance was performed to determine statistical significant difference (*, $p < 0.05$; **, $p < 0.01$; ***, $p < 0.001$). $n = 4$. *Error bars* represent the mean ± S.D.

Maintenance and Exposure of Juvenile Zebrafish—In the evening, pairs of adult zebrafish brooders were transferred to mating containers (Aquaneering). The next morning fertilized embryos were collected and divided in groups of 50 in 115-mm diameter crystallization dishes containing 100 ml of water and maintained at 28 °C. At 4 dpf, the juveniles were transferred to the circulating system. The water flow was adjusted to 20–30 drops/min, 14-h light/10-h dark cycle and fed twice with newly hatched *A. salina* nauplii and commercial flake food (Larval AP 100).

At the time of exposure, juvenile zebrafish were transferred back to crystallization dishes of 115-mm diameter with 100 ml of water (15 or 20 dpf) or 1-liter containers (180/100 mm) with 500 ml of water (41 or 70 dpf) with 20 individuals in each container. The juveniles were exposed to heat-killed *E. coli* (1×10^6, 5×10^6, 1×10^7, 5×10^7), DOC (200 μM), or NAI (20 nM). The fish were fed twice a day, and 50% of the water was changed every third day and heat-killed *E. coli*, DOC, or NAI was replenished to maintain the original concentrations. The water quality was monitored over the course of studies. The temperature was maintained at 25 ± 0.2 °C. Water pH averaged 7.3 ± 0.2, and salinity averaged 0.08 ± 0.01%. The nitrite level averaged 0.04 ± 0.05 mg/liter, whereas nitrate and ammonia level remained undetectable. Survival through the experimental exposures averaged 85 ± 5%. There was no effect of the different treatments on these parameters.

The exposures were terminated at different time points depending on the experiment and assay. For sample collection at 21 dpf, zebrafish juveniles were sacrificed by snap-freezing in liquid nitrogen and stored at −80 °C until further use. Juveniles of 35, 42, and 71 dpf of age were dissected under a stereomicroscope, and their gonads were isolated, snap-frozen in liquid nitrogen, and stored at −80 °C until further use. For sex ratio determination, the fishes were transferred back to the circulating system at the end of exposure (at 35 dpf), and the sex ratios were determined after dissection and microscopic observation of the gonads at 70 dpf.

RNA Extraction and qRT-PCR—Cells, juvenile zebrafish, and isolated gonads were homogenized in 200 μl Trizol Reagent (Sigma) and RNA was isolated according to manufacturer's instruction. cDNA synthesis was performed using qScript cDNA synthesis kit (Quanta Biosciences). Primers were designed for listed genes (supplemental Table S1). SYBR Green (Quanta) was used to determine the expression levels of all genes. Thermocycling conditions for SYBR Green consisted of a denaturation step for 5 min at 95 °C followed by 40 cycles of 95 °C for 2 s and 60 °C for 30 s. Data analysis was performed using standard curve method and ΔΔCt method (32).

Microarray-based Transcriptomics of Gonadal Samples—The gonads of 35 dpf juvenile zebrafish were isolated, and RNA was extracted from individual samples using TRIzol reagent according to manufacturer's instruction. Amplification and labeling of total RNA was performed as described previously (33) with the following modifications; 5 μg of antisense RNA was labeled with Alexa Fluor 647, whereas 20 μg of a common reference consisting of pooled antisense RNA from one individual in each treatment group (a total of 4 individuals) was labeled with Alexa Fluor 555. Microarray printing, hybridization, scanning, and data processing were performed as described previously (33). A total of 11 samples were analyzed: 6 control individuals, 3 individuals from the intermediate treatment, and 2 individuals from the highest treatment dose.

Analysis of Microarray Data—Raw expression values obtained from the GenePix Pro 6.0 software were background-corrected and normalized using R 2.9.0 (34) and the BioC limma 2.18.2 package (35, 36). Briefly, array intensity values were background corrected using the normexp method (37) followed by print-tip loess normalization within arrays and

quantile normalization between arrays. Differential expression was calculated by fitting a linear model to a group means parameterization. Multiple testing was corrected by controlling the false discovery rate (38). Principal component analysis of the normalized expression values was conducted in R using the prcomp function. The gene symbol and putative function for each EST sequence was obtained based on the best zebrafish BLAST hit against the RefSeq RNA database (as of April 12, 2011) unless indicated otherwise. The full set of microarray expression data has been deposited in ArrayExpress under the accession number E-MEXP-3249.

Testis Culture—Adult zebrafish were euthanized, and their testes were isolated. The testes were sterilized with 0.5% v/v commercial bleach in PBS (Sigma) for 2 min and washed 3 times in PBS. The testes were transferred to 24-well plate (BD Biosciences) and maintained at 28 °C and 3% CO_2 in a humidified incubator in ZFL cell media containing antibiotic-antimycotic solution (Invitrogen). The explants were cultured in parallel and exposed to heat-killed bacteria (5×10^7), DOC (200 μM), and NAI (20 nM) for 24 h.

Western Blot Analysis—The ovary samples from 71 dpf individuals were lysed in radioimmune precipitation assay buffer (150 mM NaCl, 1% Nonidet P-40, 0.5% DOC, 0.1% SDS, 50 mM Tris, pH 8) containing protease inhibitor mixture (Sigma). Protein content was quantified using Bradford reagent (Bio-Rad), and 30 μg of each sample was resolved by 12% SDS-PAGE. The proteins were transferred to a PVDF membrane (Amersham Biosciences). The membrane was incubated for 1 h in Tris-buffered saline containing 0.1% Tween to prevent nonspecific binding and probed with anti-caspase 3a antibody (AnaSpec) at 1:1000 dilution overnight. The HRP-conjugated anti rabbit IgG (Amersham Biosciences) was used at a 1:3000 dilution for 1 h, and the immunoreactive complex was detected by Super Signal West Pico chemiluminescent substrate (Thermo Scientific). The membrane was then stripped and probed for β-actin using mouse anti β-actin antibody (Sigma) at a 1:5000 dilution. The HRP-conjugated anti-mouse IgG (Amersham Biosciences) was used at 1:3000 dilution for 1 h. The bands were quantified using the ImageJ software (National Institutes of Health) and normalized with their respective β-actin level.

Statistical Analysis—Statistical significance were determined using a two-tailed non-paired Student's *t* test for two-group comparison or one-way analysis of variance followed by Dunnett post test for multiple group comparison, and differences were considered significant if the *p* values were <0.05 (*, $p < 0.05$; **, $p < 0.01$; ***, $p < 0.001$). Statistical analyses were performed using GraphPad Prism 5 software (GraphPad Software).

RESULTS

Heat-killed Escherichia coli Activate Zebrafish NF-κB Resulting in Female-biased Sex Ratios—ZFL cells stably transfected with the NF-κB-pGL4 vector (nZFL) were exposed to heat-killed *E. coli* to determine whether this would result in activation of NF-κB. A dose-dependent activation of NF-κB was observed after exposure of nZFL cells to heat-killed *E. coli* (Fig. 1*A*). The qPCR analysis also showed up-regulation of inflammatory genes like *p65*, *p50*, prostaglandin-endoperoxide synthase 2a (*ptgs2a*), interleukin 8 (*il8*), and tumor necrosis factor a (*tnfa*) in response to heat-killed *E. coli* after exposure of ZFL cells (Fig. 1, *B–F*).

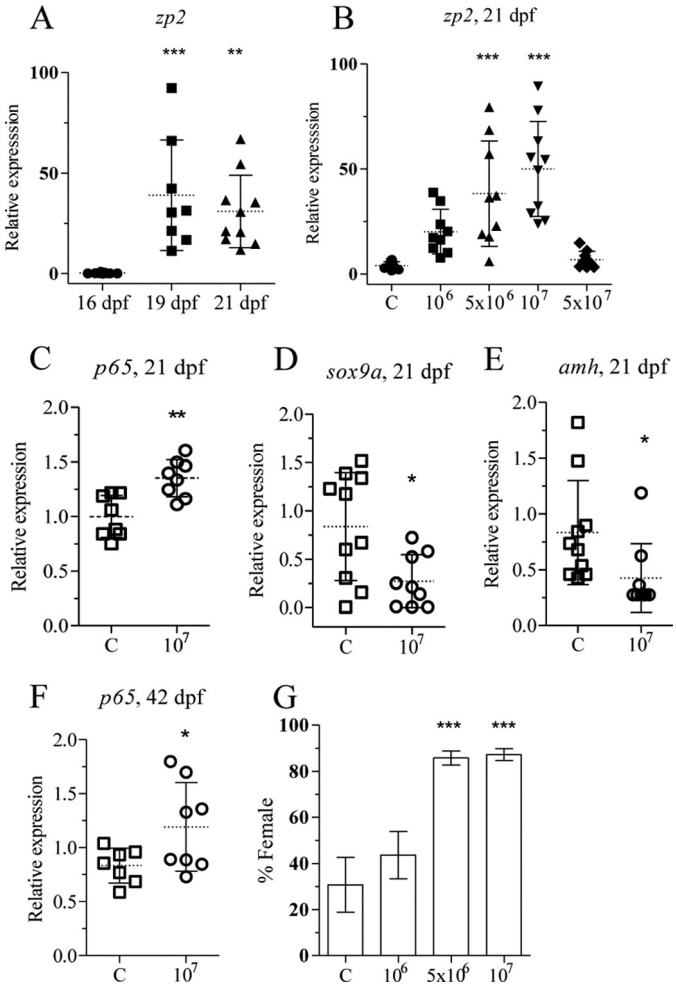

FIGURE 2. **Heat-killed *E. coli* up-regulates *p65* and *zp2* and leads to a female-biased population.** *zp2* expression was determined by qRT-PCR from individuals (16, 19, and 21 dpf) using *ef1a* and 18 S rRNA as reference genes (*A*). Zebrafish juveniles were exposed to different concentrations of heat-killed bacteria, and *zp2* expression was determined by qRT-PCR from individuals exposed from 15–21 dpf (*B*). Zebrafish juveniles at 20 and 41 dpf were exposed to heat-killed bacteria (10^7 cfu/ml) for 24 h. Analysis of *p65* (*C*), *sox9a* (*D*), and *amh* (E) expression at 21 dpf juveniles and of *p65* (*F*) expression at 42 dpf gonads was performed by qRT-PCR. Juveniles at 15 dpf were exposed to heat-killed *E. coli* for 20 days, and their sex was determined at 70 dpf. The mean and S.D. of three independent experiments is shown. Each group contained at least 20 individuals (*G*). Statistically significant differences between groups were determined using Student's *t* test for two groups and one-way analysis of variance test for more than two groups (*, $p < 0.05$; **, $p < 0.01$; ***, $p < 0.001$). *Error bars* represent the mean ± S.D.

Zebrafish juveniles are known to enter a juvenile ovary stage between 14 and 28 dpf (14, 15). This transition was indicated by the elevated levels of female-specific zona pellucida (*zp2*) gene at 19 dpf (Fig. 2*A*). Based on this information, all the exposures were started before or at the time of entry into the juvenile ovary stage.

Exposure to heat-killed bacteria from 15 to 21 dpf resulted in dose-dependent up-regulation of the *zp2* gene expression and showed a bell-shaped curve with no effect at the highest dose (Fig. 2*B*). Next, zebrafish juveniles were exposed to 1×10^7 cfu/ml heat-killed bacteria for 24 h at 20 dpf to determine

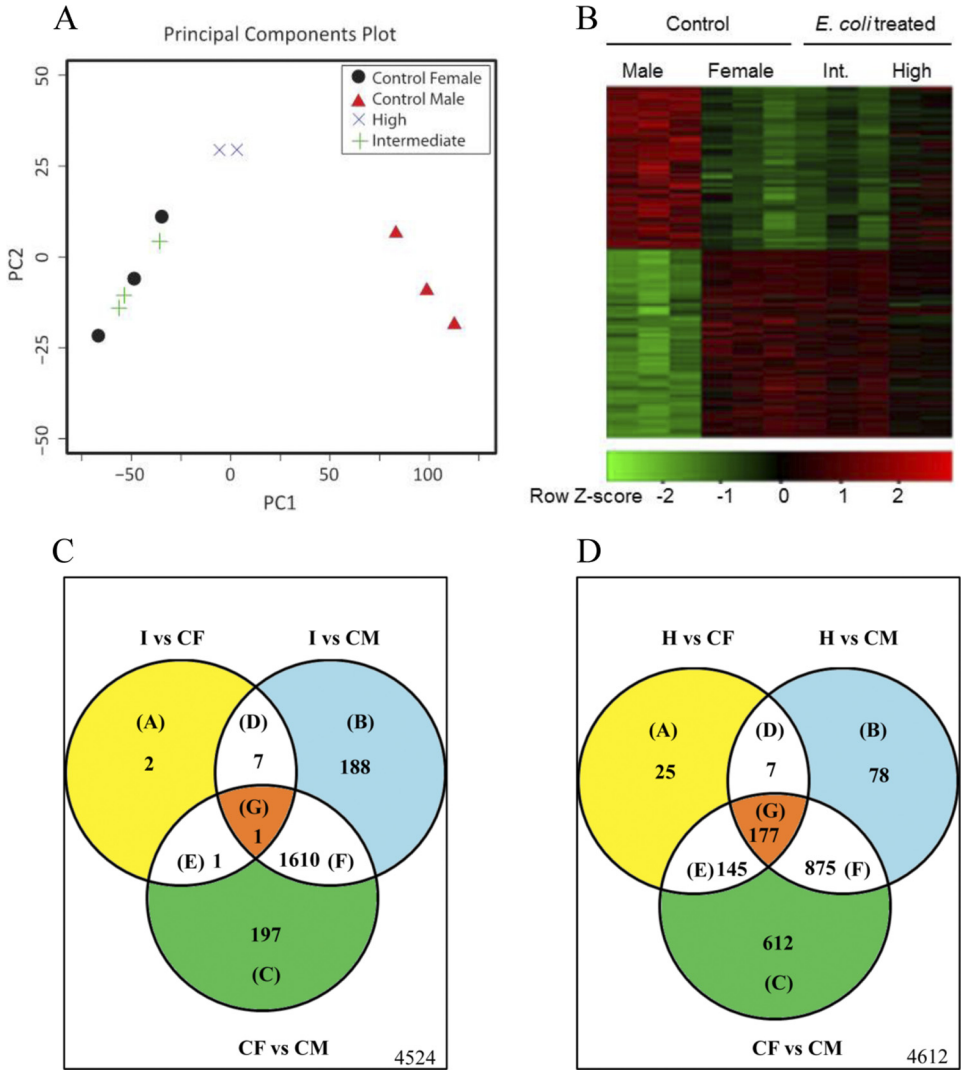

FIGURE 3. **The gonadal transcriptomes of individuals treated with heat-killed *E. coli* are similar to those of control females.** Differential gene expression was determined by a homemade gonadal cDNA microarray in the differentiating zebrafish gonads at 35 dpf after treatment with an intermediate (*Int*; 5×10^6 cfu/ml) and high dose (10^7 cfu/ml) of heat-killed *E. coli*. *A*, shown is a visualization of the main source of experimental variation using principal components analysis of all normalized array expression values. *B*, shown is a Heatmap visualization of 1812 array features differentially expressed between the control male and control female samples (-fold change ≥ 2-fold; *q* value < 0.05). *Rows* were scaled to have a mean of zero and S.D. of one. *C* and *D*, shown is a Venn analysis of genes differentially expressed (-fold change ≥ 2-fold; *q* value < 0.05) between the two sexes from the *E. coli* treatment groups and the control samples, respectively. 1) gene sets are differentially expressed after treatment with intermediate dose of heat-killed bacteria. *2*) gene sets are differentially expressed after treatment with high dose of heat-killed bacteria. *CF*, control female; *CM*, control male; *H*, high dose (10^7 cfu/ml); *I*, intermediate dose (5×10^6 cfu/ml). The number of genes that were not differentially expressed is indicated in the *lower right corner of each panel*.

whether this would result in *in vivo* up-regulation of NF-κB. The transcript level of *p65* was significantly up-regulated, whereas *sox9a* and *amh* expression were down-regulated (Fig. 2, *C–E*). This demonstrates that heat-killed bacteria induce the NF-κB pathway, similar to what is reported in mammals (28), NF-κB also down-regulates *amh* expression in zebrafish juveniles. To confirm if NF-κB activation occurred in the gonads, juveniles at 41 dpf were exposed to heat-killed bacteria for 24 h, and the gonads were excised. qRT-PCR analysis showed significant up-regulation of gonadal *p65* expression after the treatment (Fig. 2*F*). Together, these results demonstrate that treatment with heat-killed *E. coli* led to activation of NF-κB and induction of female-specific gene expression.

To determine whether treatment with heat-killed bacteria would lead to alterations in sex ratio, zebrafish juveniles were exposed to three concentrations of heat killed bacteria (1×10^6, 5×10^6 or 1×10^7 cfu/ml) during the critical period of sex differentiation (15–35 dpf). The sex ratio was determined at 70 dpf and demonstrated an increase in the proportion of females from 30 to 85% (Fig. 2*G*). These results indicated that activation of NF-κB and the inflammatory signaling pathways interfere with testis formation in zebrafish.

Microarray-based Transcriptomic Analysis Indicate the Involvement of NF-κB Pathway in the Feminization Process—A custom-printed cDNA array comprising 6370 unique gonad-derived clones (33) was used to assess changes in the gene expression landscape of juvenile zebrafish gonads in response to two different concentrations of heat-killed *E. coli* (5×10^6 and 1×10^7 cfu/ml) between 15 and 35 dpf. Principal component analysis of the normalized array expression values illustrated that exposure to heat-killed bacteria defined the main treatment effect seen in the expression data (Fig. 3*A*). Each

TABLE 1

Genes displaying the largest differential expression in gonads from juveniles exposed to intermediate levels of heat-killed *E. coli* compared to control male samples from 15–35 dpf

	Genes up-regulated in individuals treated with heat-killed bacteria			
Gene symbol	I *vs.* CM[a]	*q* Value[b]	Gene name	RefSeq ID
sinup	6.138972	3.8461E-13	Siaz-interacting nuclear protein	NM_197937
tpi1a	5.778892	1.3865E-13	Triosephosphate isomerase 1a	NM_153667
stau2	5.729454	9.1741E-13	Staufen, RNA-binding protein, homolog 2 (*Drosophila*)	NM_200925
zp3	5.513024	3.5595E-12	Zona pellucida glycoprotein 3	NM_131331
zp2.2	5.508029	3.0255E-11	Zona pellucida glycoprotein 2.2	NM_131827
cldng	5.502843	8.075E-12	Claudin g	NM_180965
snrpb	5.379755	1.1409E-14	Small nuclear ribonucleoprotein polypeptides B and B1	NM_205667
scg5	5.368851	2.5534E-12	Secretogranin V	NM_200726
mid1ip1	5.338822	1.3481E-14	MID1-interacting protein 1	NM_213439
birc5b	5.314876	5.4488E-12	Baculoviral IAP repeat-containing 5B	NM_145195
mt2	5.266296	3.5563E-12	Metallothionein 2	NM_001131053
cyc1	5.202272	1.1492E-12	Cytochrome c-1	NM_001037393
ccne	5.179989	1.6367E-15	Cyclin E	NM_130995
slc16a3	5.150553	2.3088E-15	Solute carrier family 16 member 3	NM_212708
retsatl	5.095099	1.5198E-10	Retinol saturase (all-trans-retinol 13,14-reductase)-like	NM_001040004
ccna1	5.044201	2.5394E-13	Cyclin A1	NM_212818
zp2	4.998241	9.6232E-12	Zona pellucida glycoprotein 2	NM_131330
cldnd	4.878126	1.2491E-12	Claudin d	NM_180964
thy1	4.843528	9.3008E-08	Thy-1 cell surface antigen	NM_198065
zp2l1	4.824493	1.5182E-12	Zona pellucida glycoprotein 2,-like 1	NM_001105104
zp2.2	4.618628	4.1268E-10	Zona pellucida glycoprotein 2.2	NM_131827
zar1	4.589525	6.0927E-11	Zygote arrest 1	NM_194381
col1a2	−6.30784	1.1828E-10	Collagen, type I, α2	NM_182968
col1a3	−5.40109	2.396E-11	Collagen, type I, α1b	NM_201478
cpa5	−5.1099	0.0004497	Carboxypeptidase A5	NM_199271
acta2	−4.77678	1.1754E-08	Actin, α2, smooth muscle, aorta	NM_212620
rdh1l	−4.74052	3.8436E-08	Dehydrogenase/reductase (SDR family) member 9	NM_199609
scp2	−4.74032	1.7504E-09	Sterol carrier protein 2	NM_200865
hbbe2	−4.72664	6.9984E-08	Hemoglobin β embryonic-2	NM_212846
rtn1a	−4.58485	1.8505E-08	Reticulon 1a	NM_001029967
gpx4a	−4.42594	6.1645E-06	Glutathione peroxidase 4a	NM_001007282
aldob	−4.3543	3.1299E-06	Aldolase b, fructose-bisphosphate	NM_194367
sparc	−4.2209	1.0631E-07	Secreted acidic cysteine rich glycoprotein	NM_001001942
hbae1	−4.19334	1.0071E-08	Hemoglobin α embryonic-1	NM_182940
cebpb	−3.81485	4.0853E-13	CCAAT/enhancer binding protein (C/EBP), β	NM_131884
try	−3.78429	0.00010216	Trypsin	NM_131708
acta2	−3.71892	1.0572E-09	Actin, α2, smooth muscle, aorta	NM_212620
lpl	−3.69103	3.8436E-08	Lipoprotein lipase	NM_131127
btg1	−3.69101	3.4084E-11	B-cell translocation gene 1	NM_200020
fabp3	−3.65859	9.0136E-08	Fatty acid-binding protein 3, muscle and heart	NM_152961
krt4	−3.62196	7.8536E-07	Keratin 4	NM_131509
rfc4	−3.59129	1.0284E-07	Replication factorC (activator 1) 4	NM_214737
gpx1a	−3.54498	4.1707E-07	Glutathione peroxidase 1a	NM_001007281
hbbe1	−3.53021	0.00441842	Hemoglobin β embryonic-2	NM_131759

[a] -Fold change values between the intermediate and control male groups (I *vs.* CM) have been log2-transformed.
[b] The *q* value represents the false discovery rate corrected p-value derived from the linear fit to a group means parameterization.

TABLE 2

Expression levels of genes with potential role in gonad differentiation were analyzed by microarrays using gonads from intermediate (I) doses of heat-killed *E. coli* from 15–35 dpf compared to those of control males (CM) or control females (CF)

The *q* value represents the false discovery rate-corrected *p* value derived from the linear fit to a group means paramaterization. -Fold change values between the control male and female (CF vs. CM) and the individuals treated with intermediate dose of heat-killed *E. coli* and control male (I *vs.* CM) have been log2-transformed.

Gene	CF vs. CM	*q* value	I *vs.* CM	*q* value	Name
cyp19a1a	0.116	0.675	0.146	0.594	Cytochrome P450, family 19, subfamily A, polypeptide 1a
amh	0.109	0.675	0.104	0.692	Anti-Müllerian hormone
cyp19a1b	0.063	0.856	0.028	0.939	Cytochrome P450, family 19, subfamily A, polypeptide 1b
sox9a	0.009	0.981	0.083	0.813	SRY-box containing gene 9a
foxl2	0.009	0.981	0.022	0.956	Forkhead box L2
cyp11c1	−0.391	0.136	−0.357	0.174	Cytochrome P450, family 11, subfamily C, polypeptide 1
nr5a1b	−0.176	0.498	0.013	0.965	Nuclear receptor subfamily 5, group A, member 1b
nr5a5	−0.446	0.152	−0.451	0.147	Nuclear receptor subfamily 5, group A, member 5
nr5a1a	−1.070	2.69E-06	−1.180	6.42E-07	Nuclear receptor subfamily 5, group A, member 1a

treatment group formed a tight cluster indicating no outliers among the individual transcriptomes analyzed. The results showed that individuals treated with an intermediate dose of heat-killed bacteria clustered more tightly with control females (and further apart from the control males) than the high dose group, and this may be due to the bell-shaped dose response curve observed with heat-killed bacteria (Fig. 2*B*). Sexually dimorphic expression of a selected set of genes between the control males and females is shown in the form of a heatmap (Fig. 3*B*; -fold change ≥; *q* value <0.05). Comparative analysis of the sex-specific gene expression in the treated groups revealed a striking similarity between the gonadal transcriptomic profiles of those treated with the intermediate dose and the control females, highlighting that treatment with heat-killed *E. coli*-enhanced female gonad differentiation and/or inhibited male gonad differentiation (supplemental Table S2).

TABLE 3

Analysis of differential expression of seven genes by qRT-PCR to validate microarray data

CF, control female, $n = 3$; CM, control male, $n = 2$; I, intermediate (5×10^6 cfu/ml), $n = 3$; H, high (10^7 cfu/ml), $n = 2$; MA, microarray.

Gene symbol	CF *vs.* CM		I *vs.* CM		H *vs.* CM	
	MA[a]	qPCR	MA	qPCR	MA	qPCR
bcl2	−1.34	1.53	−1.31	2.41[b]	1.09	0.64
dap3	1.57[c]	13.04[d]	1.67[c]	21.00[c]	1.17	5.49[d]
tp53	1.12	7.52[c]	1.20	14.94[d]	1.01	3.85[d]
pycard	−1.55[b]	−0.85	−1.77[b]	−0.99	1.29	−0.57
casp3a	1.4[b]	42.84[d]	1.42[b]	89.61[d]	1.05	10.82[b]
wt1a	−1.01	5.91	−1.05	7.54	1.07	3.22
zp2	40.59[c]	388.56[c]	31.96[c]	450.17[d]	17.50[c]	102.64[b]

[a] -Fold changes in gene expression for CF, I, and H compared to CM were calculated according to the formula, -fold change = ((CF, I, or H) − CM)/CM, using gonads from 35-dpf-old juveniles. Statistical significant difference from CM within a gene was determined using two-tailed Student´s *t*-test.

[b] $p < 0.05$.

[c], $p < 0.001$.

[d], $p < 0.01$.

Venn analysis was performed on the microarray data to identify genes specifically expressed in treated fish in comparison to control males and females (Fig. 3, *C* and *D*). Comparison of the gonadal transcriptome profile of the group treated with an intermediate dose with that of control females (I *versus* CF) showed that only 11 genes differed in their expression pattern between these groups (Fig. 3*C*). Two of the genes that showed differential expression were dead (Asp-Glu-Ala-Asp) box polypeptide 3 (*ddx3*), a RNA helicase involved in spermatogenesis (39), and chordin (*chd*), which plays an important role in the specification of dorsal-ventral axis during zebrafish development (40). On the other hand, 1809 genes showed significant differential expression between the gonads of individuals treated with the intermediate dose and those of the control males (*I versus CM*) (Fig. 3*C*).

Similar results were observed with the individuals treated with high dose of heat-killed bacteria, as they have also demonstrated increased female bias (Fig. 2*G*). The expression level of 354 genes (supplemental Table S3) differed between individuals

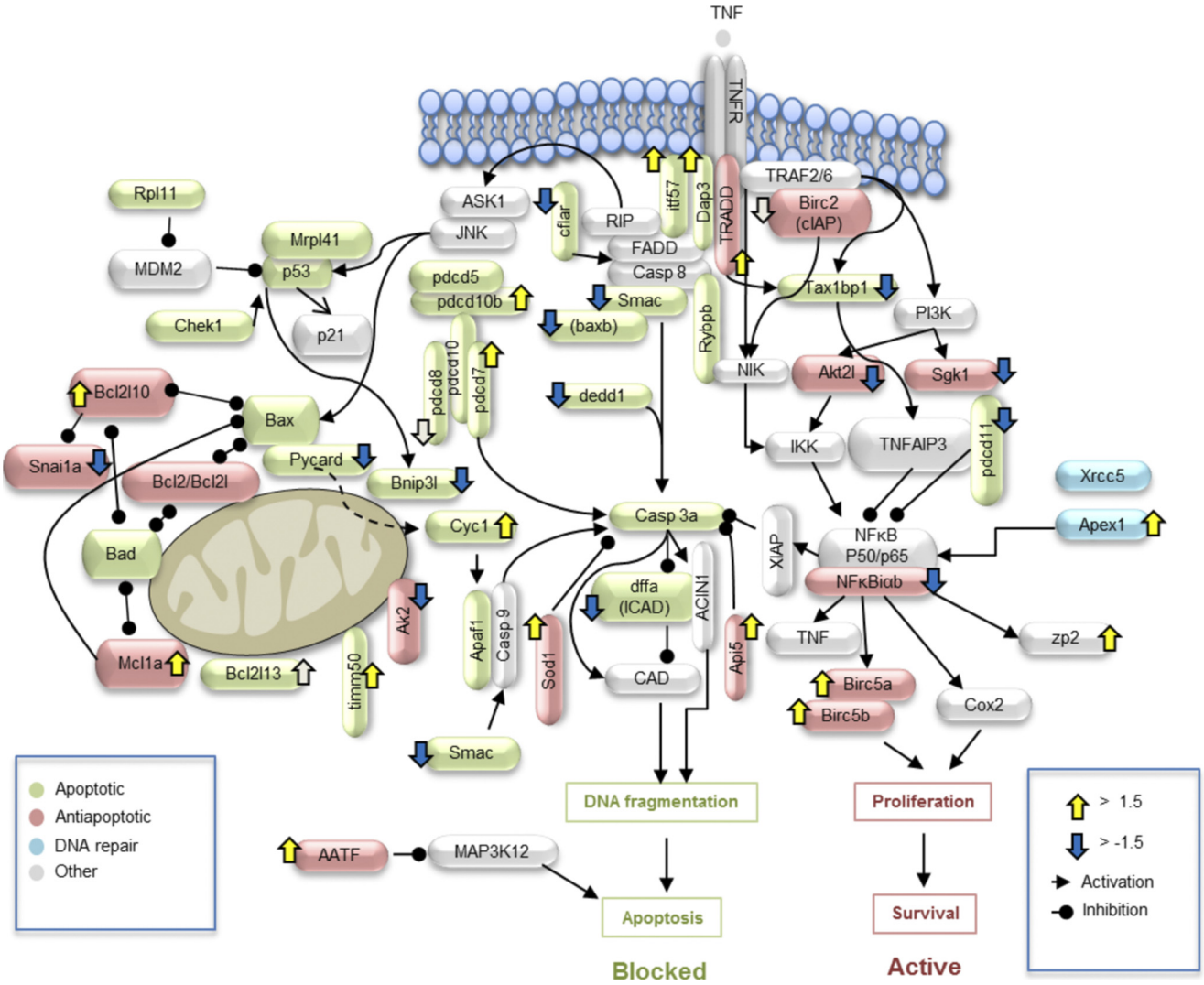

FIGURE 4. **Alteration of apoptotic/anti-apoptotic signaling by heat-killed *E. coli* treatment.** Exposure of juvenile zebrafish to an intermediate concentration (5×10^6 cfu/ml) of heat-killed *E. coli* was performed between 15 and 35 dpf. Gonads were dissected at 35 dpf. After RNA extraction, microarray was used to evaluate apoptotic and anti-apoptotic gene expression in individual gonads. Several critical apoptotic genes were suppressed (*cflar*, *dedd1*, *pycard*, *bnip3l*, and *smac*), whereas anti-apoptotic (*bcl2l10*, *aatf*, *api5*, and *mcl1a*) and NF-κB-target genes (*birc5a* and *birc5b*) were up-regulated.

TABLE 4

Apoptotic and anti-apoptotic gene expression was analyzed by microarrays in gonads of zebrafish juveniles exposed to intermediate (I) and high (H) doses of heat-killed *E. coli* from 15–35 dpf compared to those of control males (CM) or control females (CF)

The *q* value represents the false discovery rate corrected *p* value derived from the linear fit to a group means paramaterization. -Fold change values between the treated groups and controls have been log2 transformed.

Gene	CF vs. CM	*q* Value	I *vs.* CM	*q* value	Name
cyc1	5.545	4.22421E-13	5.202	1.14919E-12	Cytochrome c1
birc5b	5.458	3.48241E-12	5.315	5.44875E-12	Baculoviral IAP repeat-containing 5B
mcl1a	2.387	6.10573E-11	2.294	1.19507E-10	Myeloid cell leukemia sequence 1a
birc5a	1.804	6.38669E-08	1.778	7.91592E-08	Baculoviral IAP repeat-containing 5A
pdcd7	1.413	4.07714E-08	1.598	5.69641E-09	Programmed cell death protein 7 homolog
sod1	1.080	6.32605E-05	1.150	2.98632E-05	Superoxide dismutase
bcl2l13	0.982	0.244392481	0.323	0.732653483	Bcl-2-like 13 protein
tradd	0.945	1.72234E-06	1.006	6.88107E-07	TNFR1-associated DEATH domain protein
ift57	0.942	2.5255E-06	0.828	1.45804E-05	Intraflagellar transport protein 57
timm50	0.938	0.000141313	0.663	0.003967945	Import inner membrane translocase subunit TIM50
bcl2l10	0.725	0.000281879	0.668	0.000662021	Bcl-2-like 10 protein
pdcd10b	0.722	2.70697E-05	0.824	4.76193E-06	Programmed cell death protein 10B
dap3	0.651	0.000115272	0.741	2.46396E-05	Death- associated protein 3
aatf	0.646	0.000488524	1.026	1.65076E-06	Apoptosis-antagonizing transcription factor
apex1	0.640	0.002657661	0.905	8.01035E-05	APEX nuclease
chek1	0.569	0.002904756	0.540	0.004424879	Serine/threonine-protein kinase Chk1
pdcd5	0.497	0.003502437	0.529	0.002112974	Programmed cell death protein 5
casp3a	0.489	0.021534335	0.505	0.018007274	Caspase 3
api5	0.311	0.179674239	0.700	0.00309605	Apoptosis inhibitor 5
rybpb	0.223	0.409033765	0.143	0.618438834	Death effector domain-associated factor B
birc2	0.187	0.337374145	−0.170	0.389206313	Baculoviral IAP repeat-containing protein 2
xrcc5	0.178	0.342167521	0.232	0.206242708	X-ray repair cross-complementing protein 5
tp53	0.166	0.547499145	0.267	0.308605818	Tumor suppressor p53
pdcd10a	−0.021	0.934394561	−0.130	0.566305667	Programmed cell death protein 10A
mrpl41	−0.045	0.763067184	−0.253	0.050968156	Mitochondrial ribosomal protein L41
bax	−0.076	0.813846548	−0.169	0.581940727	Bcl-2-associated X protein
bcl2l	−0.136	0.496224495	−0.191	0.32022252	Bcl-2-like 1 protein
apaf1	−0.159	0.581732089	−0.117	0.697171658	Apoptotic protease-activating factor 1
bad	−0.334	0.215793567	−0.191	0.509176093	Bcl2 antagonist of cell death
bcl2	−0.418	0.151307689	−0.389	0.183090613	B-cell lymphoma 2
dffa	−0.537	0.001465837	−0.704	8.72749E-05	DNA fragmentation factor subunit α
pdcd8	−0.574	0.006444647	−0.680	0.001647751	Programmed cell death protein 8
pycard	−0.637	0.04378308	−0.820	0.010418878	Apoptosis-associated speck-like prot. containing CARD
nfkbiab	−0.694	0.005897655	−0.946	0.000374682	NF-κB light polypeptide gene enhancer inhibitor αb
sgk1	−1.002	0.000559778	−0.694	0.011662921	Serum/glucocorticoid-regulated kinase 1
akt2l	−1.036	0.007551645	−1.119	0.004243975	V-akt murine thymoma viral oncogene homolog 2. like
rpl11	−1.050	2.06218E-05	−1.098	1.15201E-05	60 S ribosomal protein L11
snai1a	−1.094	4.67951E-06	−1.129	3.03591E-06	Snail homolog 1a
ak2	−1.246	7.86169E-06	−1.452	9.0004E-07	Adenylate kinase isoenzyme 2
baxb	−1.343	1.49003E-07	−1.381	9.54774E-08	Bcl2-associated X protein, b
dedd1	−1.635	7.21776E-08	−1.574	1.29146E-07	Death effector domain-containing 1
smac	−1.695	0.000642094	−1.522	0.001775805	Second mitochondria-derived activator of caspase
tax1bp1	−1.841	1.8459E-08	−2.063	2.89485E-09	Tax1-binding protein 1
bnip3l	−1.941	4.97092E-09	−1.902	7.09148E-09	BCL2/adenovirus E1B 19 kDa-interacting protein 3-like
cflar	−2.585	5.34657E-11	−2.610	4.51162E-11	CASP8 and FADD-like apoptosis regulator precursor
pdcd11	−3.346	6.17826E-08	−2.841	7.32152E-07	Programmed cell death protein 11

treated with the a high dose of heat-killed *E. coli* and the control females (*H versus CF*) compared with 1138 array features differentially expressed between the high dose group and control males (*H versus CM*; Fig. 3*D*). Taken together, this indicated that the gene expression pattern elicited by heat-killed *E. coli* treatment closely resembled that of the control females as opposed to control males.

Genes showing the largest differential expression levels between individuals treated with the intermediate dose of heat-killed *E. coli* and control males (*I versus CM*) are listed in Table 1. Several of these genes, including *zp2*, *zp3*, and zygote arrest 1 (*zar1*) as well as the anti-apoptotic gene baculoviral IAP repeat-containing 5B (*birc5b*) were shown to be expressed in a female-specific manner in the treated individuals. Analysis of the differences in gene expression between control females and males and between the group treated with intermediate dose of heat-killed *E. coli* and control males showed that the expression level of *amh*, *cyp19a1a* and *b*, and cytochrome P450, family 11, subfamily C, polypeptide 1 (*cyp11c1*) did not differ between these groups at 35 dpf (Table 2). However, *zp2* showed higher expression in females and treated individuals than in males (Table 3), whereas *nr5a1a* showed higher expression in males (Table 2).

Apoptotic Signaling Pathways Are Involved in the Survival of Oocytes—To perform a more detailed assessment of the potential role of apoptotic signaling pathways in zebrafish gonad differentiation, we analyzed the expression of those genes involved in these processes that were present on the microarray. The resulting gene expression pattern was consistent with the activation of anti-apoptotic pathways and the inhibition of apoptotic pathways in response to treatment with heat-killed *E. coli* (Fig. 4; Table 4). However, a number of genes involved in apoptotic pathway remained up-regulated in both female fish and those treated with heat-killed bacteria. Several crucial pro-apoptotic genes, including direct IAP-binding protein with low phosphatidylinositol/second mitochondria-derived activator of caspase (*diablo*/*smac*), CASP8 and FADD-like apoptosis regulator (*cflar*), death effector domain-containing 1 (*dedd1),* and PYD and CARD domain containing (*pycard*) were suppressed in treated individuals compared with controls, whereas genes involved in proliferation, including two *birc5 genes* (*birc5a* and

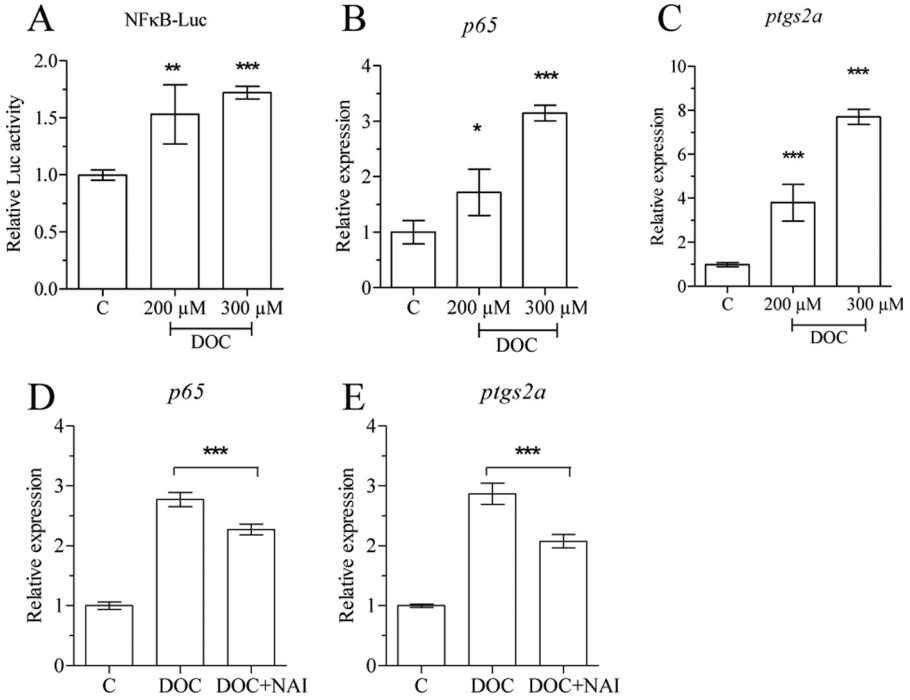

FIGURE 5. **DOC activates NFκB and up-regulates *p65* and *ptgs2a* expression *in vitro*.** nZFL were exposed to DOC (200 μM, 300 μM) for 12 h, and luciferase activity was analyzed to check NF-κB activation (*A*). ZFL cells were exposed to DOC (200 μM, 300 μM) alone and combination (200 μM DOC) with NAI (40 nM) for 24 h, and total RNA was extracted followed by qRT-PCR analysis of *p65* (*B* and *D*) and *ptgs2a* (*C* and *E*) expression. The statistically significant difference between groups was determined using Student's *t* test (*, $p < 0.05$; **, $p < 0.01$; ***, $p < 0.001$). $n = 4$. *Error bars* represent the mean ± S.D.

-b), were up-regulated (Table 4). To confirm the microarray data, the expression patterns of a selected group of genes, including B-cell leukemia/lymphoma 2 (bcl2), death associated protein 3 (*dap3*), *tp53*, *pycard*, Wilms tumor 1a (*wt1a*), and *zp2* were validated by qRT-PCR (Table 3). The obtained results confirmed the transcriptional activity profiles observed by the microarray for these genes.

Treatment with Sodium Deoxycholate Induces NF-κB Pathway Resulting in Female-biased Sex Ratios—To confirm the involvement of NF-κB in gonad differentiation, we exposed zebrafish cells and juveniles to a known NF-κB activator, DOC (41). Exposure of nZFL and ZFL cells to DOC resulted in NF-κB activation (Fig. 5*A*) and up-regulation of both *p65* and *ptgs2a* expression (Fig. 5, *B* and *C*). Exposure of zebrafish to 200 μM DOC from 15 to 21 dpf also caused an up-regulation of *p65* expression (Fig. 6*A*), whereas the levels of *sox9a*, *amh*, and *wt1a* transcripts were not significantly reduced (data not shown), suggesting that DOC triggers a weaker response than heat-killed bacteria. However, significantly up-regulated *p65* and *ptgs2a* expression (Fig. 6, *B* and *C*) was detected in the gonads of zebrafish juveniles exposed to DOC for 24 h at 41 dpf. The expression of *p65* expression was also up-regulated in testis explants in response to heat-killed bacteria and DOC (Fig. 6*D*), whereas Western blot analysis of ovary samples showed a decrease in the level of caspase 3a protein (Fig. 6*E*), confirming that the treatment inhibited gonadal apoptosis. The sex ratio was determined at 70 dpf and revealed an increased percentage of females from 25 to 45% after exposure to 200 μM DOC from 15 to 35 dpf (Fig. 6*F*).

NAI Exposure Down-regulates p65 and ptgs2a Expression Resulting in Male-biased Sex Ratios—NAI is a 6-amino-quinazoline-derived compound that is reported to inhibit NF-κB activation and TNF-α production (42). ZFL cells exposed to 200 μM DOC alone or in combination with 40 nM NAI were analyzed for *p65* and *ptgs2a* expression. NAI treatment significantly down-regulated DOC-induced *ptgs2a* and *p65* gene expression (Fig. 5, *D* and *E*). A significant down-regulation of *p65* and up-regulation of caspase 8, apoptosis-related cysteine peptidase (*casp8*), cyclin-dependent kinase inhibitor 1A (*p21*), and *smac* (Fig. 7, *A–D*) expression has been observed in juveniles exposed to 20 nM NAI for 24 h at 20 dpf. Six days of NAI exposure of zebrafish juveniles (15–21 dpf) resulted in decreased expression of *ptgs2a,* X-linked inhibitor of apoptosis (*xiap*), and *zp2* (Fig. 8, *A–C*). Exposure of juveniles to NAI for 24 h at 41 dpf resulted in reduced gonadal *ptgs2a* gene expression (Fig. 8*D*), confirming the effect of NF-κB inhibition on gonadal gene expression. Furthermore exposure of zebrafish juveniles to 20 nM NAI from 15 to 35 dpf resulted in a decreased percentage of females from 45 to 20% (Fig. 8*E*). These results further support a role of NF-κB in the maintenance of oocyte development during zebrafish sex differentiation.

DISCUSSION

Although the molecular mechanism of zebrafish sex determination remains unknown, several genes, including *sox9*, *amh*, *nr5a*, and doublesex and mab-3 related transcription factor 1 (*dmrt1*), have been proposed to be involved in the initial stages of testis and ovary differentiation (7, 8) Testis differentiation in zebrafish starts with a juvenile ovary stage followed by a transformation involving apoptotic loss of oocytes leading to the eventual development of male sex organs (14, 16). Analysis of temporal expression profile of the *zp2* gene suggests that the juvenile ovary stage is initiated before 19 dpf, indicating that all of our treatments were started before the initiation of the juve-

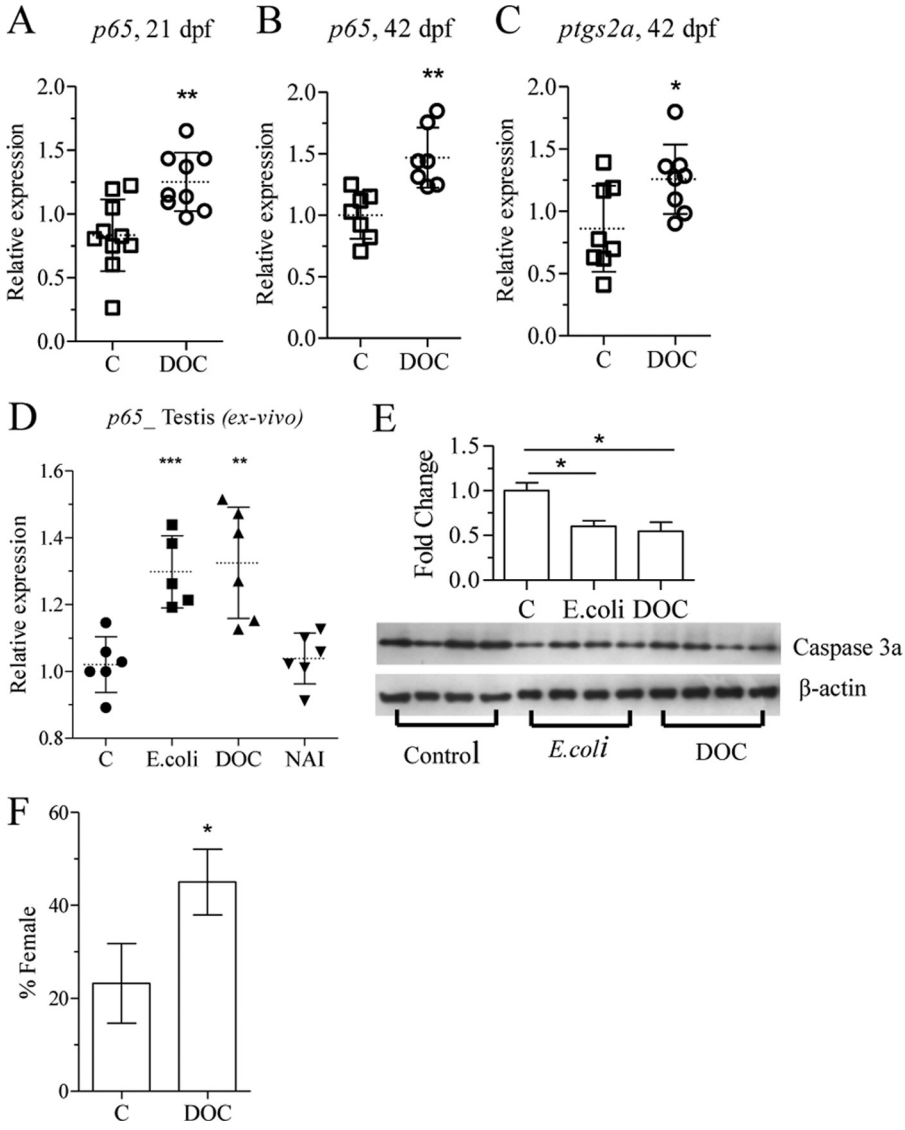

FIGURE 6. **DOC treatment up-regulates the expression of inflammatory genes leading to female-biased population.** Zebrafish juveniles were exposed to DOC (200 μM) and analyzed for changes in *p65*, *ptgs2a*, and sex ratio. Shown is analysis of *p65* levels after 6 days of exposure at 15 dpf (*A*). 24 h of exposure of 41 dpf juveniles was followed by analysis of *p65* (*B*) and *ptgs2a* (*C*) expression in the gonads. Testis explants were exposed to heat-killed bacteria (5×10^7), DOC (200 μM), and NAI (20 nM) for 24 h, and total RNA was extracted followed by qRT-PCR analysis of *p65* (*D*). Zebrafish juveniles at 70 dpf were exposed to heat-killed bacteria (5×10^7) and DOC (300 μM) for 2 days, and gonads were isolated for Western blot analysis (*E*). Larvae at 15 dpf were exposed to DOC (200 μM) for 20 days, and sex ratio was determined at 70 dpf. The mean and S.D. of two independent experiments are shown. Each group contained at least 30 individuals (*F*). Statistically significant difference between groups was determined using Student's *t* test (*, $p < 0.05$; **, $p < 0.01$; ***, $p < 0.001$). *Error bars* represent the mean ± S.D.

nile ovary stage. In this study we show that induction of gonadal inflammation, through treatment with heat-killed *E. coli* or DOC during the critical stage of gonad differentiation, activates NF-κB and anti-apoptotic signaling, resulting in maintenance of oocyte development and inhibition of testis formation. In contrast, inhibition of NF-κB activity by exposure to NAI results in an induction of testis differentiation. These results demonstrate that NF-κB is involved in the regulation of the gonadal differentiation process in zebrafish. Identifying the mechanisms of gonadal differentiation in zebrafish as well as interlinks and alterations by apoptotic and inflammatory (anti-apoptotic) responses are key factors in the understanding of possible endogenous and environmental influences during this delicate process.

NF-κB is a potent inducer of inflammatory responses as well as a modulator of apoptotic signaling (23). Several critical pro-apoptotic genes, including *smac*, *pycard*, BCL2/adenovirus E1B interacting protein-like b (*bnip3l*), and Tax1 (human T-cell leukemia virus type I)-binding protein 1b (*tax1bp1*) and *cflar*, were repressed by exposure to heat-killed *E. coli*. The decrease of caspase 3a protein levels in the ovaries confirms the anti-apoptotic effect of the treatment. The pro-apoptotic activity of these genes is well documented, and their increased expression leads to the activation of several caspases, including *casp3, casp8,* and *casp9* (43). Their roles in the activation and translocation of proteins associated with the mitochondrial apoptotic pathway have also been demonstrated (44). Furthermore, the expression of several genes with anti-apoptotic functions associated with

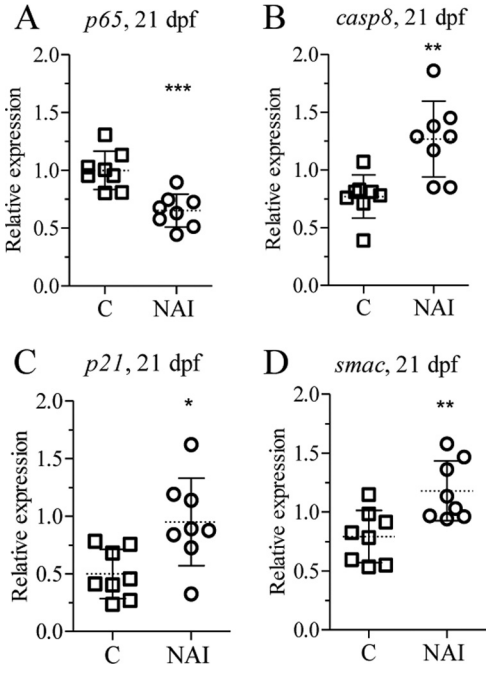

FIGURE 7. **NAI exposure alters apoptotic and anti-apoptotic gene expression *in vivo*.** Zebrafish juveniles at 20 dpf were exposed to NAI (20 nM) for 24 h and analyzed for *p65* (*A*), *casp8* (*B*), *p21* (*C*), and *smac* (*D*) transcript levels. The statistically significance difference from the control was determined using Student's *t* test (*, $p < 0.05$; **, $p < 0.01$; ***, $p < 0.001$). $n = 8$. *Error bars* represent the mean ± S.D.

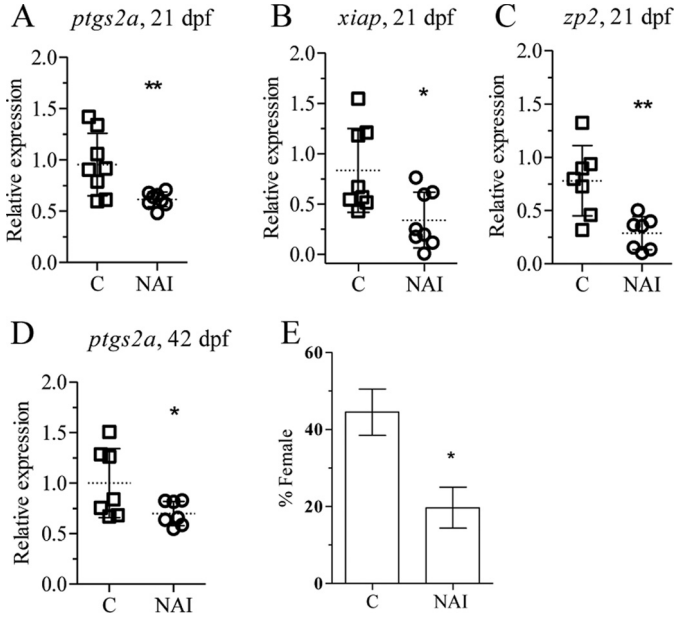

FIGURE 8. **NAI treatment down-regulates the expression of inflammatory genes leading to male-biased population.** Zebrafish juveniles were exposed to 20 nM NAI for different periods of time followed by qPCR analysis of gene expression and sex ratio. Exposure at 15 dpf for 6 days was followed by analysis of *ptgs2a* (*A*), *xiap* (*B*), and *zp2* (*C*). Zebrafish juveniles at 41 dpf were exposed for 24 h followed by qPCR analysis of *ptgs2a* (*D*). Juveniles at 15 dpf were exposed for 20 days, and the sex ratio was determined at 70 dpf (*E*). The mean and S.D. of three independent experiments are shown. Each group contained at least 30 individuals. Statistically significance difference from the control was determined using Student's *t* test (* $p < 0.05$; **, $p < 0.01$). *Error bars* represent the mean ± S.D.

NF-κB signaling, including tnfrsf1a-associated via death domain (*tradd*), *birc5a*, *birc5b*, apoptosis inhibitor 5 (*api5*), apoptosis antagonizing transcription factor (*aatf*), and myeloid cell leukemia sequence 1a (*mcl1a*), was significantly up-regulated in response to induced inflammation. In addition, expression of the NF-κB inhibitory gene nuclear factor of κ light polypeptide gene enhancer in B-cells inhibitor, αb (*nfkbiab*) was suppressed. These genes have been reported to alter apoptotic signals transduced through the extrinsic TNF receptor (45) and the intrinsic (mitochondrial) (46) pathways. This is in agreement with the observed feminization after exposure to heat-killed bacteria and DOC. To confirm the involvement of NF-κB in this process, we used NAI to block NF-κB activation.

Short term exposure of larvae to NAI down-regulated *p65*, *ptgs2a*, and *xiap* expression, whereas the activity of apoptotic genes, *smac*, *casp8*, and *p21* was significantly increased. The expression of female-specific *zp2* gene was also down-regulated, and this correlated with male-biased populations after long term exposure. Down-regulation of *zp2* and the male bias sex ratio, therefore, involves NF-κB inhibition and induction of apoptotic signals leading to oocyte apoptosis and initiation of testis differentiation. It was interesting to note that gonadal *ptgs2a* was up-regulated in DOC-treated individuals and down-regulated in NAI-treated individuals. At present, data linking prostaglandins to a direct role in sex differentiation in zebrafish are lacking. Therefore, further studies are clearly needed to elucidate the role of cyclooxygenase-2 and prostaglandins in these processes. There have been indications of the involvement of *nr5a* genes in zebrafish sex determination and gonad differentiation (8). The induction of *Amh* by Sox9, via steroidogenic factor-1, is well documented in mammals (47), but the molecular basis for gonad differentiation in zebrafish remains unclear. In this study only *nr5a1a* expression was found to be up-regulated in male fish at 35 dpf, whereas we did not observe any differential expression pattern for *cyp19a1a, cyp19a1b,* or *cyp11c1* in either control fish or after exposure to heat-killed *E. coli* from 15 to 35 dpf. This suggests that altered 17β-estradiol and 11-ketotestosterone levels are a consequence of gonad differentiation. The recent discovery of sex-associated genomic regions on chromosomes 3, 4, 5, and 16 (5, 6) makes it unlikely that zebrafish would have a classical sex determination system. Instead, the interplay between different loci may be instrumental to the development of testis or ovary in the species (4, 7). As the identified regions account only for some of the variance, it is likely that other genes are also involved in the process.

Zebrafish gonad differentiation involves a juvenile ovary stage after which the gonad either receives signals to maintain differentiating oocytes or to induce oocyte apoptosis and trigger the transformation into a testis structure. The correlation between NF-κB activity and sex differentiation shown in this study is in good agreement with earlier studies suggesting the involvement of apoptosis and tp53 in testis development (16, 17). Further research is needed to elucidate the sex-specific signaling pathways leading to the regulation of NF-κB activity in zebrafish during the juvenile ovary stage, thereby controlling the further development into the ovary and testis.

REFERENCES

1. Sola, L., and Gornung, E. (2001) Classical and molecular cytogenetics of the zebrafish, *Danio rerio* (Cyprinidae, Cypriniformes). An overview. *Genetica* **111,** 397–412
2. Wallace, B. M., and Wallace, H. (2003) Synaptonemal complex karyotype of zebrafish. *Heredity* **90,** 136–140
3. Singer, A., Perlman, H., Yan, Y., Walker, C., Corley-Smith, G., Brandhorst, B., and Postlethwait, J. (2002) Sex-specific recombination rates in zebrafish (*Danio rerio*). *Genetics* **160,** 649–657
4. Liew, W. C., Bartfai, R., Lim, Z., Sreenivasan, R., Siegfried, K. R., and Orban, L. (2012) Polygenic sex determination system in zebrafish. *PLoS One* **7,** e34397
5. Bradley, K. M., Breyer, J.P., Melville, D.B., Broman, K.W., Knapik, E.W., and Smith, J.R. (2011) An SNP-based linkage map for zebrafish reveals sex determination loci. *G3* **1,** 3–9
6. Anderson, J. L., Rodríguez Marí, A., Braasch, I., Amores, A., Hohenlohe, P., Batzel, P., and Postlethwait, J. H. (2012) Multiple sex-associated regions and a putative sex chromosome in zebrafish revealed by RAD mapping and population genomics. *PLoS One* **7,** e40701
7. Orban, L., Sreenivasan, R., and Olsson, P. E. (2009) Long and winding roads. Testis differentiation in zebrafish. *Mol. Cell. Endocrinol.* **312,** 35–41
8. von Hofsten, J., and Olsson, P. E. (2005) Zebrafish sex determination and differentiation. Involvement of FTZ-F1 genes. *Reprod. Biol. Endocrinol.* **3,** 63
9. Siegfried, K. R., and Nüsslein-Volhard, C. (2008) Germ line control of female sex determination in zebrafish. *Dev. Biol.* **324,** 277–287
10. Rodríguez-Marí, A., Yan, Y. L., Bremiller, R. A., Wilson, C., Cañestro, C., and Postlethwait, J. H. (2005) Characterization and expression pattern of zebrafish *anti-Müllerian hormone* (*amh*) relative to *sox9a*, *sox9b*, and *cyp19a1a* during gonad development. *Gene Expression Patterns* **5,** 655–667
11. Lasala, C., Carré-Eusèbe, D., Picard, J. Y., and Rey, R. (2004) Subcellular and molecular mechanisms regulating anti-Müllerian hormone gene expression in mammalian and nonmammalian species. *DNA Cell Biol.* **23,** 572–585
12. Arango, N. A., Lovell-Badge, R., and Behringer, R. R. (1999) Targeted mutagenesis of the endogenous mouse *Mis* gene promoter. *In vivo* definition of genetic pathways of vertebrate sexual development. *Cell* **99,** 409–419
13. Wagner, T., Wirth, J., Meyer, J., Zabel, B., Held, M., Zimmer, J., Pasantes, J., Bricarelli, F. D., Keutel, J., Hustert, E., Wolf, U., Tommerup, N., Schempp, W., and Scherer, G. (1994). *Cell* **79,** 1111–1120
14. Takahashi, H. (1977) Juvenile Hermaphroditism in the Zebrafish, *Brachydanio rerio*. *Bull. Fac. Fish. Hokkaido Univ.* **28,** 57–65
15. Wang, X. G., Bartfai, R., Sleptsova-Freidrich, I., and Orban, L. (2007) The timing and extent of "juvenile ovary" phase are highly variable during zebrafish testis differentiation. *J. Fish Biol.* **70,** 33–44
16. Uchida, D., Yamashita, M., Kitano, T., and Iguchi, T. (2002) Oocyte apoptosis during the transition from ovary-like tissue to testes during sex differentiation of juvenile zebrafish. *J. Exp. Biol.* **205,** 711–718
17. Rodríguez-Marí, A., Cañestro, C., Bremiller, R. A., Nguyen-Johnson, A., Asakawa, K., Kawakami, K., and Postlethwait, J. H. (2010) Sex reversal in zebrafish fancl mutants is caused by Tp53-mediated germ cell apoptosis. *PLoS Genet.* **6,** e1001034
18. Slanchev, K., Stebler, J., de la Cueva-Méndez, G., and Raz, E. (2005) Development without germ cells. The role of the germ line in zebrafish sex differentiation. *Proc. Natl. Acad. Sci. U.S.A.* **102,** 4074–4079
19. Siebenlist, U., Franzoso, G., and Brown K. (1994) Structure, regulation, and function of NF-κB. *Annu. Rev. Cell Biol.* **10,** 405–455
20. Ghosh, S., and Hayden, M. S. (2008) New regulators of NF-κB in inflammation. *Nat. Rev. Immunol.* **8,** 837–848
21. Xiao, W. (2004) Advances in NF-κB signaling transduction and transcription. *Cell. Mol. Immunol.* **1,** 425–435
22. Finco, T. S., and Baldwin, A. S (1995) Mechanistic aspects of NF-κB regulation. The emerging role of phosphorylation and proteolysis. *Immunity* **3,** 263–272
23. Aggarwal, B. B., Sethi, G., Nair, A., and Ichikawa, H. (2006) Nuclear factor-κB. A holy grail in cancer prevention and therapy. *Curr. Signal Transduct. Ther.* **1,** 25–52
24. Srinivasula, S. M., and Ashwell, J. D. (2008) IAPs. What's in a name? *Mol. Cell* **30,** 123–135
25. Rao, N. A., McCalman, M. T., Moulos, P., Francoijs, K. J., Chatziioannou, A., Kolisis, F. N., Alexis, M. N., Mitsiou, D. J., and Stunnenberg, H. G. (2011) Coactivation of GR and NF-κB alters the repertoire of their binding sites and target genes. *Genome Res.* **21,** 1404–1416
26. Palvimo, J. J., Reinikainen, P., Ikonen, T., Kallio, P. J., Moilanen, A., and Jänne O. A. (1996) Mutual transcription interference between Rel A and androgen receptor. *J. Biol. Chem.* **271,** 24151–24156
27. Delfino, F., and Walker, W.H. (1998) Stage-specific nuclear expression of NF-κB in mammalian testis. *Mol. Endocrinol.* **12,** 1696–1707
28. Hong, C. Y., Park, J. H., Seo, K. H., Kim, J. M., Im, S. Y., Lee, J. W., Choi, H. S., and Lee, K. (2003) Expression of *MIS* in the testis is down-regulated by tumor necrosis factor α through the negative regulation of SF-1 transactivation by NF-κB. *Mol. Cell. Biol.* **23,** 6000–6012
29. Murakami, S., Lefebvre, V., and de Crombrugghe, B. (2000) Potent inhibition of the master chondrogenic factor Sox9 gene by interleukin-1 and tumor necrosis factor-α. *J. Biol. Chem.* **275,** 3687–3692
30. Meijer, A. H., van der Sar, A. M., Cunha, C., Lamers, G. E., Laplante, M. A., Kikuta, H., Bitter, W., Becker, T. S., and Spaink, H. P. (2008) Identification and real-time imaging of a myc-expressing neutrophil population involved in inflammation and mycobacterial granuloma formation in zebrafish. *Dev. Comp. Immunol.* **32,** 36–49
31. Lister, A., and Van Der Kraak, G. (2002) Modulation of goldfish testicular testosterone production *in vitro* by tumor necrosis factor a, interleukin-1β, and macrophage conditioned media. *J. Exp. Zool.* **292,** 477–486
32. Schmittgen, T. D., and Livak, K.J. (2008) Analyzing real-time PCR data by the comparative C_T method. *Nat. Protoc.* **3,** 1101–1108
33. Sreenivasan, R., Cai, M., Bartfai, R., Wang, X., Christoffels, A., and Orban, L. (2008) Transcriptomic analyses reveal novel genes with sexually dimorphic expression in the zebrafish gonad and brain. *PLoS One* **3,** e1791
34. Ihaka, R., and Gentleman, R. (1996) R: A language for data analysis and graphics. *J. Comput. Graph. Stat.* **5,** 299–314
35. Smyth, G. K. (2004) Linear models and empirical bayes methods for assessing differential expression in microarray experiments. *Stat. Appl. Genet. Mol. Biol.* **3,** 3
36. Smyth, G. K., and Speed, T. (2003) Normalization of cDNA microarray data. *Methods* **31,** 265–273
37. Ritchie, M. E., Silver, J., Oshlack, A., Holmes, M., Diyagama, D., Holloway, A., and Smyth, G. K. (2007) A comparison of background correction methods for two-color microarrays. *Bioinformatics* **23,** 2700–2707
38. Benjamini, Y., and Hochberg, Y. (1995) Controlling the false discovery rate. A practical and powerful approach to multiple testing. *J. R. Stat. Soc. B* **57,** 289–300
39. Sekiguchi, T., Iida, H., Fukumura, J., and Nishimoto, T. (2004) Human DDX3Y, the Y-encoded isoform of RNA helicase DDX3, rescues a hamster temperature-sensitive ET24 mutant cell line with a DDX3X mutation. *Exp. Cell Res.* **300,** 213–222
40. Gilardelli, C. N., Pozzoli, O., Sordino, P., Matassi, G., and Cotelli, F. (2004) Functional and hierarchical interactions among zebrafish vox/vent homeobox genes. *Dev. Dyn.* **230,** 494–508
41. Payne, C. M., Weber, C., Crowley-Skillicorn, C., Dvorak, K., Bernstein, H., Bernstein, C., Holubec, H., Dvorakova, B., and Garewal, H. (2007) Deoxycholate induces mitochondrial oxidative stress and activates NF-κB through multiple mechanisms in HCT-116 colon epithelial cells. *Carcinogenesis* **28,** 215–222
42. Tobe, M., Isobe, Y., Tomizawa, H., Nagasaki, T., Takahashi, H., and Hayashi, H. (2003) A novel structural class of potent inhibitors of NF-κB activation. Structure-activity relationships and biological effects of 6-aminoquinazoline derivatives. *Bioorg. Med. Chem.* **11,** 3869–3878
43. Shiozaki, E. N., and Shi, Y. (2004) Caspases, IAPs, and Smac/DIABLO: Mechanisms from structural biology. *Trends Biochem. Sci.* **39,** 486–494
44. Ohtsuka, T., Ryu, H., Minamishima, Y. A., Macip, S., Sagara, J., Nakayama, K. I., Aaronson, S. A., and Lee, S. W. (2004) ASC is a Bax adaptor and regulates the p53-Bax mitochondrial apoptosis pathway. *Nat. Cell Biol.* **6,**

121–128
45. Hsu, H., Xiong, J., and Goeddel, D.V. (1995) The TNF receptor 1-associated protein TRADD signals cell death and NF-κB activation. *Cell* **81,** 495–504
46. Rigou, P., Piddubnyak, V., Faye, A., Rain, J. C., Michel, L., Calvo, F., and Poyet, J. L. (2009) The antiapoptotic protein AAC-11 interacts with and regulates Acinus-mediated DNA fragmentation. *EMBO J.* **28,** 1576–1588
47. Lasala, C., Schteingart, H. F., Arouche, N., Bedecarrás, P., Grinspon, R. P., Picard, J.Y., Josso, N., di Clemente, N., and Rey, R. A. (2011) SOX9 and SF1 are involved in cyclic AMP-mediated up-regulation of anti-Müllerian gene expression in the testicular prepubertal Sertoli cell line SMAT1. *Am. J. Physiol. Endocrinol. Metab.* **301,** E539–E547